AIAA JOURNAL
Vol. 36, No. 4, April 1998

Fatigue of Cracked Plates Repaired with Single-Sided Composite Patches

T. Y. Kam,* K. H. Chu,† and Y. C. Tsai†
National Chiao Tung University, Hsin Chu 300, Taiwan, Republic of China

Fatigue of cracked plates repaired with single-sided composite patches is studied via both analytical and experimental approaches. A finite element model, which considers out-of-plane bending effects induced by asymmetric repair, is presented to determine the crack tip opening displacements of the repaired plates subjected to in-plane loading. The modified crack closure technique is used to calculate the stress intensity factor of the repaired plates. Fatigue life of the repaired plates is studied via the use of Paris law for crack propagation. The effects of cracked plate and composite patch thicknesses on the fatigue crack propagation of repaired plates containing different types of cracks are investigated. Fatigue tests of aluminum C-T specimens repaired with single-sided composite patches are performed, and the test data are used to validate the analytical approach. It has been shown that the repair of a cracked plate with a single-sided composite patch may have beneficial or adverse effects on the fatigue life of the repaired plate depending on the thicknesses of the patch and the cracked plate.

Introduction

DUE to many merits of composites, repair of cracked or aging structures with bonded composite patches has shown great promise to become a viable method for life extension of such structures. In recent years, many researchers have studied different aspects of repair with bonded composite patches.[1–11] A number of researchers have proposed different numerical techniques for stress analysis and the subsequent derivation of stress intensity factor of repaired structures.[2–8] For instance, Sun et al.[6] developed a finite element model for analyzing the stress distribution and stress intensity factor of cracked plates repaired with a single-sided patch. On the other hand, several investigators have studied the fatigue behavior of cracked structures repaired with bonded composite patches.[9–11] For instance, Baker[10] studied the fatigue crack propagation of centrally cracked aluminum panels patched with boron/epoxy composites. Most of the previous work on fatigue behavior of repaired plates, however, has been concentrated on the fatigue of double-sided repairs or single-sided repairs but without considering the out-of-plane bending effect induced by the asymmetric patching. It is not difficult to realize that the bending effect induced in a repaired plate with a single-sided patch will introduce additional tension in the cracked plate, which will then reduce the effectiveness of the patching repair. Thus, the neglect of the out-of-plane bending effect may mistakenly underestimate the stress intensity factor and lead to unconservative fatigue life prediction for the repaired plate.

In this paper, a method is presented to study the fatigue crack propagation of cracked plates repaired with a single-sided composite patch. The method includes out-of-plane bending effects for the repaired plates subjected to in-plane loading. The composite patch is assumed to be perfectly bonded to the cracked plate. Fatigue tests of C-T specimens of various thicknesses repaired with single-sided composite patches of different thicknesses are performed, and the test results are used to verify the accuracy of the proposed method. The effects of patch or plate thicknesses on fatigue crack propagation of repaired plates containing different types of cracks are studied via the present method.

Stress Intensity Factor

The stress intensity factor of a cracked plate repaired with a single-sided composite patch is determined in a finite element analysis. To illustrate the finite element formulation, consider the plate in Fig. 1, which contains a center crack of size $2a$ and is repaired with a single-sided composite patch via adhesive bonding. Herein, the cracked plate and the composite patch are treated as Mindlin plates that have the following displacement fields:

$$\begin{aligned} u^\alpha(x, y, z) &= u_0^\alpha(x, y) + z\psi_x^\alpha(x, y) \\ v^\alpha(x, y, z) &= v_0^\alpha(x, y) + z\psi_y^\alpha(x, y) \\ w^\alpha(x, y, z) &= w_0^\alpha(x, y), \qquad \alpha = c, p \end{aligned} \tag{1}$$

where x, y, and z are the local reference coordinates for the plate or patch; u_0, v_0, and w_0 are midplane displacements; ψ_x and ψ_y are shear rotations; and the superscripts $\alpha = c, p$ stand for the cracked plate and patch, respectively. In the finite element model, the cracked plate is modeled by four-noded plate elements, the composite patch four-noded quadrilateral and/or three-noded triangular plate elements, and the adhesive layer three-dimensional rectangular brick elements of eight nodes and/or triangular solid elements of six nodes. The aspect ratio of the three-dimensional brick elements is chosen in such a way that no numerical instability will occur. The compatibility conditions at the interfaces between the cracked plate (or the composite patch) and the adhesive layer are observed by enforcing the following constrained equations:

$$\underline{u}^a(x, y, -h_a/2) = \underline{u}^c(x, y, h_c/2) \tag{2}$$

and

$$\underline{u}^a(x, y, h_a/2) = \underline{u}^p(x, y, -h_p/2) \tag{3}$$

where $\underline{u}^a = (u^a, v^a, w^a)$ are displacements of the adhesive layer; and h_c, h_a, and h_p, are thicknesses of the cracked plate, adhesive layer, and patch, respectively. The commercial finite element code NASTRAN[12] is used to accomplish the preceding finite element analysis. The compatibility conditions of Eqs. (2) and (3) are handled by using the command ZOFFS in the finite element code. The command ZOFFS performs the task of offsetting the midplane of the plate elements to a distance of half-plate (or half-patch) thickness from the bottom (or top) surface of the three-dimensional brick elements.

The modified crack closure technique[13,14] is used to determine the mode I stress intensity factor of the repaired plate. Figure 2 shows a two-dimensional finite element model for the cracked plate near the crack tip at point B. If the crack extension Δa is small, e.g., Δa is less than 0.42% and 0.1% of crack size a for the edge and center crack problems, respectively, the crack opening displacements at node B can be taken to be the same as those at node A. The strain energy release rate, which is defined as the work done by the nodal

Received April 8, 1997; revision received Dec. 10, 1997; accepted for publication Jan. 5, 1998.

*Professor, Department of Mechanical Engineering. Member AIAA.
†Graduate Student, Department of Mechanical Engineering.

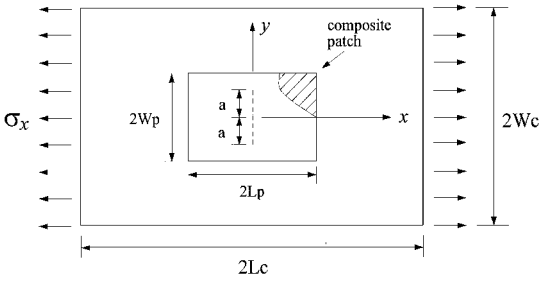

Fig. 1 Centrally cracked plate repaired with a single-sided composite patch.

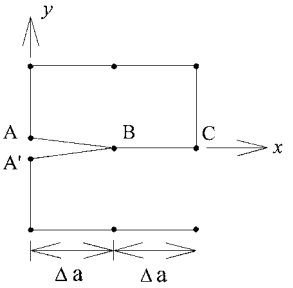

Fig. 2 Top view of plate elements around crack tip.

forces in closing the crack opening displacements, at the crack front on the unpatched surface is assumed to be expressed as the sum of two parts, i.e.,

$$G_{IR} = G_{IU} + G_{I\Psi} \tag{4}$$

with

$$G_{IU} = (1/2\Delta a)\left[F_y^B(v^A - v^{A'})\right] \tag{5a}$$

$$G_{I\Psi} = (1/2\Delta a)\left[M_x^B(\Psi_y^A - \Psi_y^{A'})\right] \tag{5b}$$

where G_{IR} is the total strain energy release rate; G_{IU} and $G_{I\Psi}$ are the strain energy release rates induced by the in-plane nodal force and nodal moment, respectively; F_y and M_x are in-plane nodal force and nodal moment, respectively; and the superscript denotes node point. Similarly, the mode I stress intensity factor K_{IR} on the unpatched surface of the repaired plate can be written as the sum of two parts, i.e.,

$$K_{IR} = K_{IU} + K_{I\Psi} \tag{6}$$

with

$$K_{IU} = \sqrt{\frac{G_{IU}E_c}{h_c}} \tag{7a}$$

$$K_{I\Psi} = \sqrt{\frac{3G_{I\Psi}E_c}{h_c}} \tag{7b}$$

where E_c is Young's modulus of the cracked plate. It is noted that the validity of the modified crack closure technique for stress intensity factor predictions of plates with single-sided repair modeled by plate elements has been demonstrated by Sun et al.[6] In their study, they also showed that for a crack with symmetric fracture surface with respect to the midplane of the cracked plate the distribution of stress intensity factor through the thickness of a cracked plate repaired with a single-sided patch is nearly linear. Herein, the suitability of the modified crack closure technique for fatigue fracture analysis of cracked plates repaired with a single-sided composite patch will be studied, and the validity of the assumption of linear distribution of the stress intensity factor through plate thickness will be investigated.

Fatigue Crack Propagation

The Paris law[13] of crack propagation is used to study the fatigue behaviors of cracked plates with and without repairs:

$$\frac{da}{dN} = C(\Delta K)^m \tag{8}$$

where N is the number of the fatigue cycle; C and m are material constants; and ΔK is the difference between the maximum ($K_{\max}$) and minimum ($K_{\min}$) values of the stress intensity factor during a fatigue cycle. The stress intensity factors of the crack front on the unpatched surface of the cracked plate with single-sided repair are used to determine ΔK in the fatigue analysis of the repaired plate. Because the cracked plate is modeled by two-dimensional plate elements, the crack front is implicitly assumed to be symmetric with respect to the midplane of the plate and the effects induced by the asymmetric fracture surface are neglected in the fatigue analysis. It is noted that for a hot-cured composite patch repair, the induced residual thermal stresses in the repaired plate may affect the effective loading ratio $R(= K_{\max}/K_{\min})$, which in turn affects the value of the material constant C in Eq. (8). Nevertheless, in view of the repair method, it is reasonable to assume that the residual thermal stresses on the unpatched side of the repaired plate are small and they have little effect on the effective loading ratio R of the unpatched surface. Thus, based on the preceding assumption, the value of material constant C for an unpatched plate can still be used for the fatigue analysis of a patched plate. The integration of Eq. (8) yields the fatigue life N_f of the cracked structure,

$$N_f = \int_{a_0}^{a_f} \frac{da}{C(\Delta K)^m} \tag{9}$$

where a_0 and a_f are the initial and final crack lengths, respectively. It is noted that the magnitude of ΔK may depend on crack length. Thus a series of finite element analyses of the cracked plate with different crack lengths is performed to trace the history of ΔK. Once the values of ΔK at different crack lengths are available, Eq. (9) is then solved via the numerical integration method of the Gauss–Kronrod rule[15] to yield N_f.

Experimental Approach

Fatigue tests of cracked aluminum C-T specimens repaired with single-sided composite patches of different thicknesses were performed to validate the analytical approach. The C-T specimens were made of 7075-T7351 aluminum and manufactured in accordance with standards[16] of the American Society of Testing and Materials. The composite patches were made of graphite/epoxy (Q-1115) prepreg tapes supplied by the Toho Co. of Japan. The adhesive was composed of MB1113 structure resin and 6762 base resin supplied by Narmco of the United States. The properties of the aluminum plate, the graphite/epoxy lamina, and the adhesive layer are listed in Table 1. The C-T specimens without repair were first precracked to the size of $a \cong 30$ mm. The crack size was determined via visual inspection with the assistance of a microscope. Several of the precracked C-T specimens were then repaired asymmetrically with a composite patch via the following cure cycle: temperature 120°C, pressure 40 psi, and curing time 1 h. The dimensions of the repaired specimens are shown in Fig. 3. The distance l is 25 mm for $h_p = 0.3$, 0.6, and 0.9 mm or 20 mm for $h_p = 1.2$ mm. The patch is made of several unidirectional graphite/epoxy laminae with fiber direction perpendicular to the crack. Herein, one specimen was made for each type of repair. Specimens of thickness $h_c = 12.7$ mm (6.35 mm) with and without repairs were subjected to cyclic load of mean 3300 N (2200 N), amplitude 2700 N (1800 N), and frequency 4 Hz via a 10-ton Instron testing machine. The fracture surfaces of the aluminum plates with single- or double-sided repairs are shown in Fig. 4 for comparison. It is noted that the fracture surface of the aluminum plate with the single-sided repair is asymmetric with respect to the midplane of the plate. It is obvious that the crack on the patched surface is shorter than that on the unpatched surface of the repaired

Table 1 Properties of specimen and bonded composite patch

Aluminum plate	$h_c = 12.7$ mm, $E = 71.7$ GPa, $\nu = 0.33$, $C = 2.714 \times 10^{-8}$, $m = 3.158$
Adhesive	$E = 2.702$ GPa, $\nu = 0.4$, $h_a = 0.102$ mm
Gr/Ep ply	$E_1 = 132.5$ GPa, $E_2 = 7.9$ GPa $G_{12} = 4.2$ GPa, $G_{23} = 1.02$ GPa $\nu_{12} = 0.28$, $h = 0.15$ mm

Table 2 Experimental fatigue life of repaired C-T specimens

Patch thickness, mm	Fatigue life, cycles $h_c = 12.7$ mm, $\bar{P} = 3300$ N	Fatigue life, cycles $h_c = 6.35$ mm, $\bar{P} = 2200$ N
0	23,281	9,385
0.3	29,900	65,300
0.6	20,403	——
0.9	17,000	45,688
1.2	15,000	——

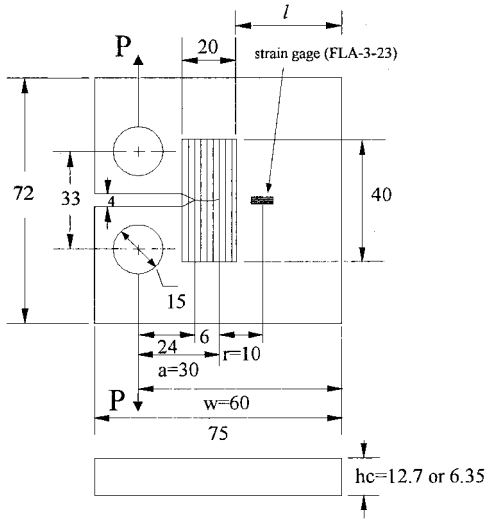

Fig. 3 Cracked C-T specimen repaired with bonded composite patch. (Units are in millimeters.)

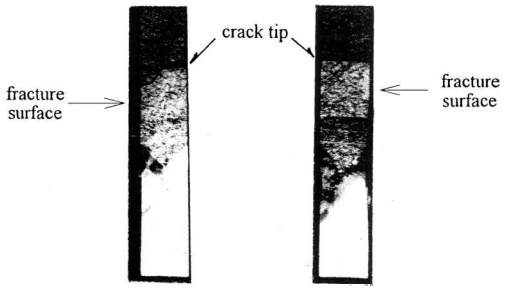

Fig. 4 Fracture surfaces of aluminum plate with single- or double-sided repairs.

specimen. The development of an asymmetric fracture surface is mainly due to the nonuniform distribution of ΔK across plate thickness. From experimental observations, the crack size of the unpatched surface dominates the fatigue life of the repaired specimen. The whole specimen will fail when the crack on the unpatched surface reaches its critical value. The fatigue lives of the specimens repaired with single-sided patches of different thicknesses for a crack propagating from $a_0 = 3.0$ mm to $a_f = 40$ mm are listed in Table 2. It is noted that for the specimens of thickness $h_c = 12.7$ mm only the bonded composite repair with a patch of thickness $h_p = 0.3$ mm was able to extend the fatigue life of the cracked specimen and the increase in patch thickness would cause adverse effects on the fatigue life of the specimens, i.e., a thicker patch yielded a shorter fatigue life. When the thickness of the specimen reduced to 6.35 mm, the out-of-plane bending effect became less obvious and both the bonded composite repairs of $h_p = 0.3$ and 0.9 mm could extend the fatigue life of the cracked specimen. The beneficial effect, however, dwindled as the patch thickness increased.

Results and Discussion

The fracture behavior of the aforementioned C-T specimens repaired with a single-sided composite patch is analyzed using the proposed finite element model. Because the stress intensity factor determined via the modified crack closure method depends on the value of the crack tip element size Δa in Fig. 2, it is worth studying the relation between the stress intensity factor and Δa before proceeding to the fatigue study of the repaired specimens. A series of finite element analyses of the C-T specimens of thickness $h_c = 12.7$ mm repaired with a single-sided composite patch of $h_p = 0.0, 0.3$, and 1.2 mm is performed using different values of Δa. The case of $h_p = 0.0$ mm is for the C-T specimen without repair. A typical finite element mesh of the repaired specimen is shown in Fig. 5. The results of the convergence tests on the normalized stress intensity factor of the unpatched surface for the specimens with different crack sizes, $a = 30$ and 35 mm, are listed in Tables 3 and 4, respectively. Herein, the normalized stress intensity factor for the edge crack problem is defined as

$$\bar{K}_I = \frac{K_I}{(P/h_c\sqrt{w})f(\beta)} \tag{10}$$

with

$$\beta = a/w$$

and

$$f(\beta) = \frac{(2+\beta)(0.886 + 4.64\beta - 13.32\beta^2 + 14.72\beta^3 - 5.6\beta^4)}{(1-\beta)^{\frac{3}{2}}}$$

It is noted that the normalized stress intensity factors for the cases without repair tend to converge as $\Delta a \leq 0.125$ mm, where the error is less than 1%. As for the cases with repair, the difference between the normalized stress intensity factor of $\Delta a = 0.125$ mm and the one of $\Delta a = 0.625$ mm is less than 0.5%. In view of the convergence test results, it is thus reasonable to choose $\Delta a = 0.125$ mm in the finite element analysis of the repaired C-T specimens. It is noted that the results presented in Tables 3 and 4 also indicate the beneficial and adverse effects of the repairs with 0.3 and 1.2 mm composite patches, respectively. The out-of-plane bending effects on the stress intensity factor of the repaired specimens with different crack lengths are to be further studied. The relations between the stress intensity factor and the crack length with or without the considerations of the out-of-plane bending effects for the C-T specimens of thickness $h_c = 12.7$ mm repaired with a single-sided composite patch of $h_p = 0.3$ and 1.2 mm are shown in Figs. 6 and 7, respectively. The stress intensity factor K_{Ir} of the repaired specimens without the consideration of the out-of-plane bending effect

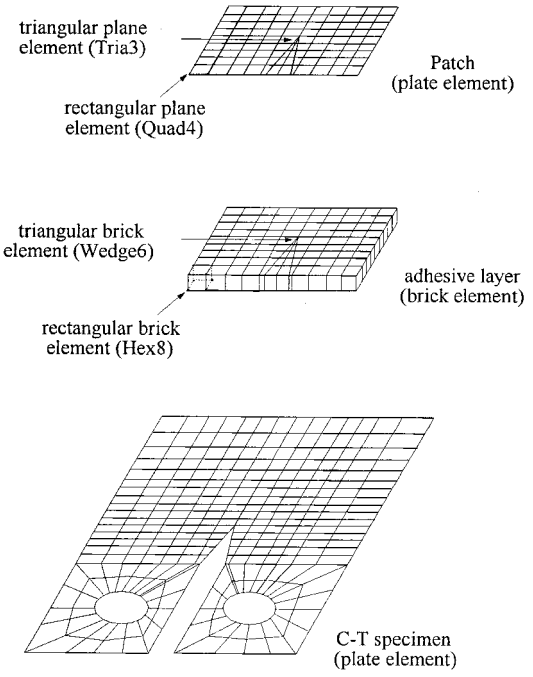

Fig. 5 Finite element model for repaired C-T specimen.

Table 3 Normalized stress intensity factor vs Δa for repaired C-T specimens with different patch thicknesses (a = 30 mm and P = 5400 N)

	Patch thickness, mm					
	0.0 (without patch)		0.3		1.2	
Δa, mm	Normalized SIF I	Error, $\left[\frac{1.0-\text{I}}{1.0}\right]$%	Normalized SIF II	Error, $\left[\frac{0.9446-\text{II}}{0.9446}\right]$%	Normalized SIF III	Error, $\left[\frac{1.2262-\text{III}}{1.2262}\right]$%
1.0000	0.9733	2.67	0.9273	1.8315	1.2019	1.9817
0.5000	0.9818	1.82	0.9339	1.1328	1.2125	1.1173
0.2500	0.9861	1.39	0.9366	1.0564	1.2152	0.8971
0.1250	0.9910	0.90	0.9405	0.4340	1.2209	0.4322
0.0625	0.9956	0.40	0.9446	——	1.2262	——

Table 4 Normalized stress intensity factor vs Δa for repaired C-T specimens with different patch thicknesses (a = 35 mm and P = 5400 N)

	Patch thickness, mm					
	0.0 (without patch)		0.3		1.2	
Δa, mm	Normalized SIF I	Error, $\left[\frac{1.0-\text{I}}{1.0}\right]$%	Normalized SIF II	Error, $\left[\frac{0.9642-\text{II}}{0.9642}\right]$%	Normalized SIF III	Error, $\left[\frac{1.2521-\text{III}}{1.2521}\right]$%
1.0000	0.9738	2.62	0.9493	1.5453	1.2298	1.7810
0.5000	0.9826	1.74	0.9545	1.0060	1.2399	0.9744
0.2500	0.9873	1.27	0.9565	0.7986	1.2439	0.6549
0.1250	0.9923	0.77	0.9602	0.4340	1.2470	0.4073
0.0625	0.9971	0.29	0.9642	——	1.2521	——

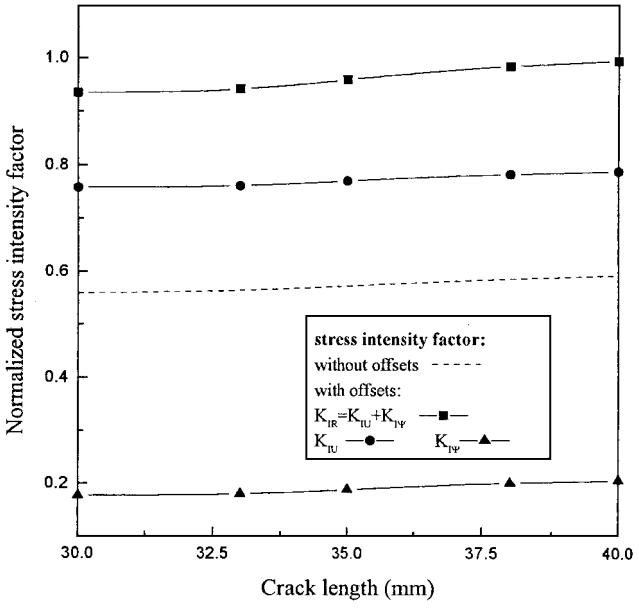

Fig. 6 Stress intensity factors of C-T specimen repaired with a 0.3-mm patch determined by different methods.

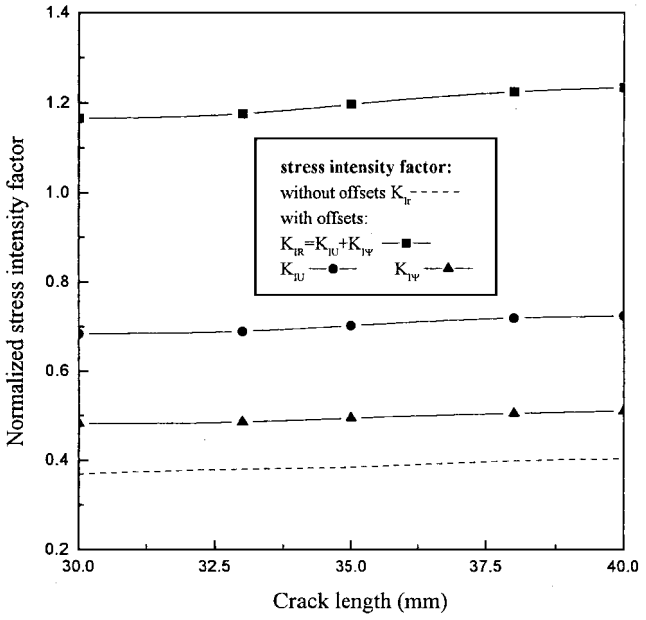

Fig. 7 Stress intensity factors of C-T specimen repaired with a 1.2-mm patch determined by different methods.

is determined by assuming zero entries for the command ZOFFS in the finite element modeling of the cracked plate and patch. The force applied to the specimens is $P = 5000$ N. Figure 6 shows the beneficial effect of single-sided repair where the repair with a two-layered patch reduces the normalized stress intensity factor of the C-T specimen without repair. Nevertheless, $\bar{K}_{IU}$ is about four times larger than $\bar{K}_{I\Psi}$, and thus the stress intensity factor of the repaired specimen is dominated by the in-plane stress intensity factor. It is also noted that the finite element model without the inclusion of the out-of-plane bending effect (zero offsets for the plate and patch) underestimates the normalized stress intensity factor of the repaired specimen. The stress intensity factor of the repaired specimen increases gradually as the crack grows in size. On the contrary, Fig. 7 shows an ill-chosen single-sided repair scheme in which the repair of the specimen with an eight-layered patch increases the stress intensity factor of the specimen without repair. Again the stress intensity factor of the repaired specimen increases gradually as the crack grows in size. Compared with the preceding example of the two-layered patch repair, the gap between $\bar{K}_{IU}$ and $\bar{K}_{I\Psi}$ for this case becomes smaller ($\bar{K}_{IU} \approx 1.4\bar{K}_{I\Psi}$), and this demonstrates the importance of the out-of-plane bending effect. Furthermore, the neglect of the bending effects induced by the thicknesses of the cracked plate and patch (no offsets for the plate and patch) in the finite element modeling also yields erroneous predictions of the normalized stress intensity factor for the repaired specimen as manifested by the fact that $\bar{K}_{IR}$ (with offset) is at least three times larger than $\bar{K}_{Ir}$ (without offset). Now consider the fatigue life of the repaired specimens of two different thicknesses, $h_c = 12.7$ and 6.35 mm, predicted by the present analytical method using the material properties listed in Table 1. The fatigue lives of the repaired specimens with a crack propagating from $a_0 = 30$ mm to $a_f = 40$ mm are listed in Table 5. For comparison purpose, the

Table 5 Theoretical fatigue life of repaired C-T specimens[a]

	$h_c = 12.7$ mm		$h_c = 6.35$ mm	
Patch thickness, mm	Theoretical fatigue life, cycles	Difference, $\left\lvert\frac{\text{experimental} - \text{theoretical}}{\text{experimental}}\right\rvert$ %	Theoretical fatigue life, cycles	Difference, $\left\lvert\frac{\text{experimental} - \text{theoretical}}{\text{experimental}}\right\rvert$ %
0	23,545	1.11	9,293	0.98
0.15	34,136	——	72,764	——
0.30	27,185	9.080	61,147	6.35
0.60	21,502	5.386	——	——
0.90	15,568	8.424	41,442	9.29
1.20	13,623	9.180	——	——

[a]Experimental fatigue life is listed in Table 2.

Table 6 Normalized stress intensity factor vs Δa for a center-cracked plate repaired with different patch thicknesses (a = 25 mm)

	Patch thickness, mm					
	0.0 (without patch)		0.254		0.762	
Δa, mm	Normalized SIF I	Error, $\left[\frac{1.0 - \text{I}}{1.0}\right]$ %	Normalized SIF II	Error, $\left[\frac{0.8240 - \text{II}}{0.8240}\right]$ %	Normalized SIF III	Error, $\left[\frac{0.9770 - \text{III}}{0.9770}\right]$ %
1.0000	0.9571	4.29	0.7619	7.5364	0.9161	6.2287
0.5000	0.9617	3.83	0.7835	4.9150	0.9357	4.2210
0.2500	0.9667	3.33	0.7960	3.3981	0.9487	2.8966
0.1000	0.9809	1.91	0.8144	1.7159	0.9661	1.1132
0.0500	0.9891	1.09	0.8215	0.3034	0.9750	0.2148
0.025	0.9918	0.82	0.8240	——	0.9770	——

differences between the theoretical and experimental fatigue lives are calculated and also listed in Table 5. It is noted that the present analytical method can predict reasonably accurate fatigue life with an error less than 10% for the repaired specimens. Thus, the stress intensity factor on the unpatched surface predicted by the modified crack closure method together with Paris law is, in a macroscopic sense, suitable for fatigue analysis of cracked plates with single-sided repairs. In the present study, the optimal patch thicknesses for the specimens of $h_c = 12.7$ and 6.35 mm are 0.15 mm (one-layer patch). Next it is worth studying the validity of the assumption of the linear distribution of the stress intensity factor through the plate thickness for a fatigue crack. As expected, the crack sizes of the patched and unpatched surfaces predicted separately by the present method are different, and thus the fracture surface of the crack becomes asymmetric with respect to the midplane of the cracked plate. This phenomenon has also been observed from experiment as indicated in Fig. 4. Nevertheless, the comparative study between experimental and theoretical predictions of the crack size of the patched surface shows that the difference between the theoretical and experimental predictions may be too big to be overlooked. For instance, when the crack growth on the unpatched surface of the repaired specimen with $h_c = 12.7$ mm and $h_p = 0.3$ mm is 14 mm, the theoretical and experimental predictions of the crack growth on the patched surface are 4.37 and 8.00 mm, respectively, and hence the theoretical prediction is 45% less than the experimental prediction. The inability of the present finite element model in producing an accurate crack size for the patched surface of the repaired plate can be attributed to the existence of the nonlinear distribution of the stress intensity factor through the plate thickness. Local factors such as the unsymmetry of the fracture surface, the residual thermal stresses, the local debonding of the adhesive layer, etc., are likely to be responsible for the development of the nonlinear distribution of the stress intensity factor through the plate thickness. Nevertheless, these local factors have less effects on the unpatched than on the patched surfaces of the repaired plate. If an accurate description of the growth of the crack surface is desired, the cracked plate must be modeled by three-dimensional elements instead of plate elements and all local effects taken into account in the fatigue analysis.

The fracture behavior of the centrally cracked plate repaired with a single-sided composite patch in Fig. 1 is studied. A typical finite element mesh for the centrally cracked plate with the single-sided repair is shown in Fig. 8. The material properties and plate dimensions used in the analysis are listed as follows:

Table 7 Normalized stress intensity factors for single-sided repair of centrally cracked plate (Δa = 0.025 mm)

		Sun et al.[6]		
Location	Present study	Plate model	Three-dimensional FEM	Chue et al.[7]
Midplane $\bar{K}$	0.567	0.536	0.612	0.481
Free surface $\bar{K}$	0.977	0.953	0.985	0.902

cracked aluminum plate, $E_c = 71.02$ GPa and $\nu_c = 0.32$; dimensions $L_c = 180$ mm, $W_c = 120$ mm, and $h_c = 2.29$ mm; boron composite patch, $E_1 = 208$ GPa, $E_2 = 25.44$ GPa, $G_{12} = G_{13} = 7.24$ Pa, $G_{23} = 4.94$ Pa, and $\nu_{12} = 0.1677$; dimensions $L_p = 76$ mm, $W_p = 38$ mm, and $h_p = 0.762$ mm; adhesive, $G_a = 0.965$ GPa, $\nu_a = 0.32$, and $h_a = 0.1016$ mm; and crack length: $a = 25$ mm. The normalized stress intensity factor for the center crack problem is defined as

$$\bar{K}_I = \frac{K_I}{\sigma_x \sqrt{\pi a}} \tag{11}$$

where σ_x is the loading stress in the x direction. After a thorough convergence test as shown in Table 6, the size of the crack tip element in Fig. 2 is set as $\Delta a = 0.025$ mm, for which the error is less than 1% for different types of single-sided repair. The normalized stress intensity factors at the midplane and the free surface of the aluminum plate are listed in Table 7 in comparison with those obtained by other researchers.[6,7] It is noted that the present solutions of the stress intensity factors at the midplane and free surface are better than those obtained by Sun et al.[6] using the plate model. Fatigue crack propagation of the centrally cracked aluminum plate of various thicknesses repaired with a single-sided composite patch of different thicknesses subjected to cyclic stress of mean 0.5 MPa and amplitude 0.5 MPa is studied using the values of the crack propagation parameters, C and m, in Table 1. Figure 9 shows the normalized fatigue lives for the repaired plate of two different plate thicknesses, $h_c = 2.29$ or 3.5 mm. It is noted that the repair of the centrally cracked aluminum plate of thickness $h_c = 2.29$ mm with a single-sided composite patch of thickness falling within the range under consideration ($h_p \leq 0.762$ mm) can yield beneficial effects on the fatigue life of the cracked plate. The beneficial effects, however, start to dwindle as $h_p > 0.127$ mm (one layer patch) and may eventually cause an adverse effect on the fatigue life of the cracked plate when $h_p > 0.762$ mm (six-layer patch). A similar phenomenon has

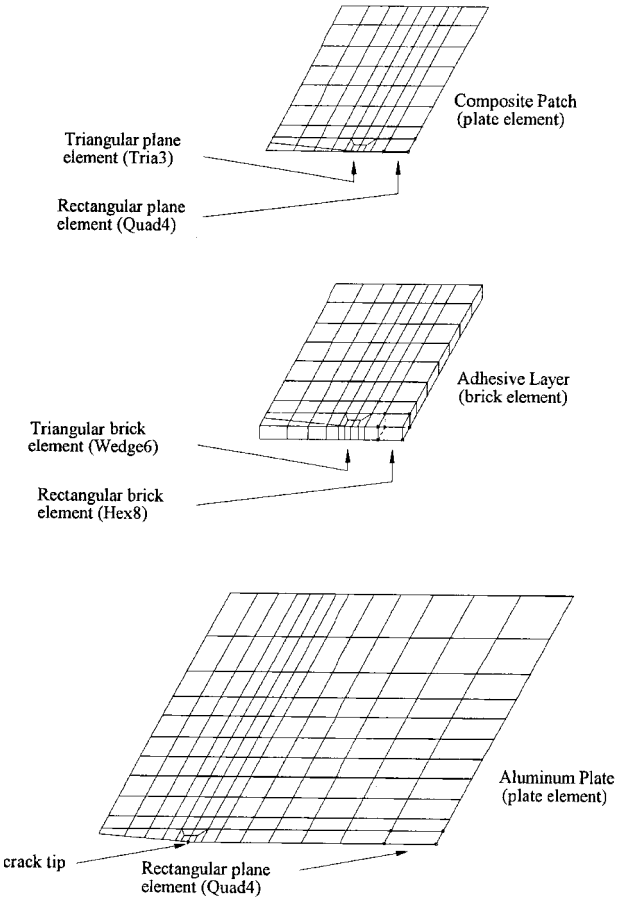

Fig. 8 Finite element model of a quarter of the repaired aluminum plate.

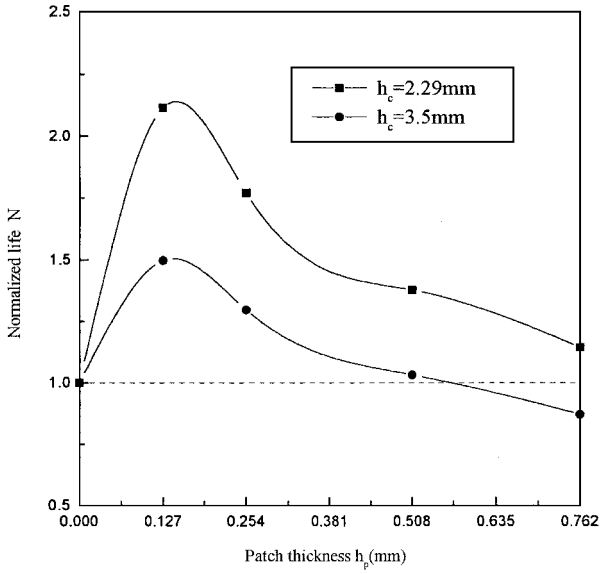

Fig. 9 Fatigue life of centrally cracked plate with single-sided repair.

also been observed for the repair of the cracked plate of thickness $h_c = 3.5$ mm where the adverse effect on the fatigue life of the cracked plate is destined to occur when the thickness of the patch is greater than 0.508 mm (four-layer patch).

Conclusion

Analytical and experimental methods were used to study the fracture and fatigue behaviors of cracked plates repaired with a single-sided composite patch. Fatigue tests of aluminum C-T specimens of various thicknesses repaired with a single-sided composite patch of different thicknesses were carried out. The importance of the out-of-plane bending effect of the single-sided repair was manifested via the fatigue life data of the repaired specimens. A finite element model was presented to simulate the mechanical behavior of cracked plates repaired with a single-sided composite patch. Fundamental fracture mechanics techniques were used in the finite element analysis to predict the stress intensity factor and the fatigue life of the repaired plates. The accuracy of the present analytical method in predicting the fatigue life of repaired plates was verified by the test data. The application of the present analytical method in predicting the stress intensity factor and the fatigue life of repaired plates was demonstrated by means of the repair of a centrally cracked plate. The out-of-plane bending effect induced by the asymmetric repair of the centrally cracked plate was also studied. It has been shown that both plate and patch thicknesses might play important roles on fatigue life of the cracked plate with an asymmetric repair. The present finite element method, however, is inadequate to predict the actual behavior of the fracture surface of a fatigue crack in a plate with single-sided repair. Further study is required if a more realistic prediction of microscopic fatigue behavior of cracked plates with single-sided repair is desired.

Acknowledgment

This research was supported by the National Science Council of the Republic of China under Grant NSC 85-2212-E009-016.

References

[1]Baker, A. A., and Jones, R., *Bonded Repair of Aircraft Structure*, Martinus–Nijhoff, Dordrecht, The Netherlands, 1988, pp. 1–214.

[2]Young, A., Cartwright, D. J., and Rooke, D. P., "The Boundary Element Method for Analyzing Repair Patches on Cracked Finite Sheets," *Aeronautical Journal of the Royal Aeronautical Society*, Vol. 92, No. 920, 1988, pp. 416–421.

[3]Young, A., Cartwright, D. J., and Rooke, D. P., "Analysis of Patched and Stiffened Cracked Panels Using the Boundary Element Method," *International Journal of Solids Structures*, Vol. 29, No. 17, 1992, pp. 2201–2216.

[4]Park, J. H., Ogiso, T., and Atluri, S. N., "Analysis of Crack in Aging Aircraft Structures with and without Composite-Patch Repairs," *Computational Mechanics*, Vol. 10, Nos. 3 and 4, 1992, pp. 169–201.

[5]Young, A., Rooke, D. P., and Cartwright, D. J., "Numerical Study of Balanced Patch Repairs to Cracked Sheets," *Aeronautical Journal of the Royal Aeronautical Society*, Vol. 93, Nov. 1989, pp. 327–333.

[6]Sun, C. T., Klug, J., and Arendt, C., "Analysis of Cracked Aluminum Plates Repaired with Bonded Composite Patches," *AIAA Journal*, Vol. 34, No. 2, 1996, pp. 369–374.

[7]Chue, C. H., Chang, L. C., and Tsai, J. S., "Bonded Repair of a Plate with Inclined Central Crack Under Biaxial Loading," *Composite Structures*, Vol. 28, No. 1, 1994, pp. 39–45.

[8]Lin, S. C., Chu, R. C., and Lin, Y. S., "A Finite Element Model for Single-Sided Crack Patching," *Engineering Fracture Mechanics*, Vol. 46, No. 6, 1993, pp. 1005–1021.

[9]Ratwani, M. M., "Characterization of Fatigue Crack Growth in Bonded Structures," Air Force Flight Dynamics Lab., AFFDL-TR-77-31, Vols. 1 and 2, Wright–Patterson AFB, OH, June 1977.

[10]Baker, A. A., "Fatigue Crack Propagation Studies on Aluminum Panels Patched with Boron/Epoxy Composite," *International Conference on Aircraft Damage Assessment and Repair* (Melbourne, Australia), edited by R. Jones and N. J. Miller, Inst. of Engineers, Melbourne, Australia, 1991, pp. 209–215.

[11]Leibovich, H., Sasson, N., Simon, A., and Green, A. K., "Repair of Cracked Aluminum Aircraft Structure with Graphite/Epoxy Patches," *Proceedings of 9th International Conference on Composite Materials* (Madrid, Spain), edited by A. Miravete, Vol. 4, Woodhead Publishing, Cambridge, England, UK, 1993, pp. 461–468.

[12]"MSC/NASTRAN Version 66," MacNeal-Schwendler Corp., Los Angeles, CA, Dec. 1990.

[13]Broek, D., *Elementary Engineering Fracture Mechanics*, Noordhoff International, Leyden, The Netherlands, 1974, pp. 260–298.

[14]Young, M. J., and Sun, C. T., "On the Strain Energy Release Rate for a Cracked Plate Subjected to Out-of-Plane Bending Moment," *International Journal of Fracture*, Vol. 60, No. 2, 1993, pp. 227–247.

[15]"IMSL User's Manual," IMSL, Inc., Houston, TX, Dec. 1989.

[16]"ASTM Standard E399-78a, Plane Strain Fracture Toughness of Metallic Materials," *Annual Book of ASTM Standards*, Vol. 02.02, American Society of Testing and Materials, 1978.

A. M. Waas
Associate Editor